

Identification of MARCO and PCSK6 As Key Genes Promoting Hepatic Metastasis in Pancreatic Cancer via Bioinformatics Analysis

Hang He (✉ hhe10@fudan.edu.cn)

Huashan Hospital Fudan University <https://orcid.org/0000-0002-5481-8794>

Minrui Liang

Huashan Hospital Fudan University

Research Article

Keywords: MARCO, PCSK6, immune microenvironment, tumor metabolism

Posted Date: February 3rd, 2022

DOI: <https://doi.org/10.21203/rs.3.rs-1303593/v1>

License:   This work is licensed under a Creative Commons Attribution 4.0 International License.

[Read Full License](#)

Abstract

Background: Hepatic metastasis occurred frequently in pancreatic cancer and leads to a poor prognosis. Genes promoting hepatic metastasis would help finding out the way to improve survivals of patients.

Methods and results: GSE42952 and GSE71729 out of 181 data serials from Gene Expression Omnibus (GEO) with samples of both hepatic metastasis and primary tumor of pancreatic cancer were chosen to generate differentially expressing genes (DEGs). 217 up-regulated and 257 down-regulated genes overlapped between the two data serials and were defined as hepatic metastasis related DEGs (H-DEGs), among which 27 up-regulated and 2 down-regulated H-DEGs were verified by both tumor tissues and cell lines of pancreatic cancer. Gene ontology (GO) and KEGG pathway analysis were performed and showed reprogramming of tumor metabolism might promote hepatic metastasis. The prognostic significance of H-DEGs were investigated. Up-regulation of MARCO and PCSK6 were both correlated to decreased overall survivals in pancreatic cancer. Immune cell infiltration analysis indicated MARCO involved in regulating tumor immune microenvironment. Gene set enrichment analysis found PCSK6 was related to activations of critical pathways and regulation of glycolysis.

Conclusions: MARCO and PCSK6 might promote hepatic metastasis of pancreatic cancer via modulating tumor immune microenvironment and tumor metabolism respectively.

Introduction

Pancreatic cancer was one of the most aggressive and malignant tumors in alimentary system [1]. The 5-year survival rate for patients with pancreatic cancer was less than 10% despite great advance in diagnosis and therapeutic regimen [2]. Liver was one of the most common sites of distant metastasis and hepatic metastasis was a major reason for impeding curative resections of pancreatic cancer [3]. Investigation of the genes promoting hepatic metastasis will provide unique biomarkers for early diagnosis and promising molecules for targeting therapies, to improve the overall survivals of patients with pancreatic cancer [4, 5].

Process of hepatic metastasis consisted of several stages including detachment of tumor cell from primary tumor, dissemination of tumor cell through circulation and settlement in liver [6]. Previous studies had found a series of novel genes and canonical pathways driving tumor progression, via microarray analysis or high throughput sequencing with samples of tumor tissue, peripheral blood or tumor cell line [7-9], however the understanding of hepatic metastasis of pancreatic cancer remained inadequate.

Tumor cell gaining or losing biological properties were dependent on the microenvironment during the process of metastasis and accompanied by variation of expression profile [10, 11]. Due to heterogeneity of primary tumor and dynamic change of microenvironment, investigation of DEGs between primary tumor and adjacent normal tissue may not focus on the genes most correlated to hepatic metastasis of pancreatic cancer.

In this study, we made a comparison between samples of hepatic metastasis and primary tumor to find out key genes related to hepatic metastasis. The generated DEGs were further verified with data from public database and analyzed through online tools or R packages. Promising genes were identified and interaction networks were established to explore the potential functions and downstream signaling pathways.

Materials And Methods

Microarray data

Data serials were collected from GEO (www.ncbi.nlm.nih.gov/geo/), a public functional genomics data repository. The searching criteria was defined as pancreatic cancer OR pancreatic tumor OR pancreatic ductal adenocarcinoma (keyword), Homo sapiens (organisms), and expression profiling by array (study type). Data serials including samples of both hepatic metastasis and primary tumor from surgical resections were chosen for further analysis.

Identification of DEGs

Genes expressing in samples of hepatic metastasis were compared to genes expressing in samples of primary tumor in each data serial to generate DEGs respectively by GEO2R (www.ncbi.nlm.nih.gov/geo/geo2r), using the parameters including adjusted p value and Benjamini & Hochberg (False discovery rate). Log transformation was applied to the data. DEGs with $\text{Log}_2 \text{FC} \geq 1$ or ≤ -1 and adjusted p value < 0.05 were considered as statistically significant. DEGs from each data serial were analyzed to obtain overlapped genes by Venn diagrams (bioinformatics.psb.ugent.be/webtools/Venn), which were presented as up-regulated and down-regulated DEGs respectively.

Validation of DEGs in tumor tissues and cell lines

Both up-regulated and down-regulated DEGs were validated in samples of primary tumor compared to samples of adjacent normal tissue from the Cancer Genome Atlas (TCGA) and GTEx through an online tool GEPIA2 (gepia2.cancer-pku.cn/#index). Adjusted p value < 0.01 and $\text{Log}_2 \text{FC} \geq 1$ or ≤ -1 were defined as cutoff values.

To exclude the influence of mesenchymal components, the obtained DEGs were verified in cell lines of pancreatic cancer from Cancer Cell Line Encyclopedia (CCLE) through an online tool DepMap Portal (depmap.org/portal/). The mRNA expressing profiles of 13 cell lines from CCLE (ASPC1, BXPC3, CAPAN1, CAPAN2, CFPAC1, HPAC, HPAFII, HS766T, MIAPACA2, PANC1, SU8686, SUIT2, SW1990) were applied. The mRNA expression of each gene was presented as Transcripts Per Kilobase Million (TPM). $\text{Log}_2(\text{TPM}+1) < 2$ was defined as negative expression. The DEGs in previous step with $\text{Log}_2(\text{TPM}+1) < 2$ in all 13 cell lines were excluded. The verified DEGs were presented by heat plot using an online tool Heatmapper (www.heatmapper.ca/).

GO and KEGG pathway analysis of DEGs

R package clusterProfiler and org.Hs.eg.db were employed to performed GO and KEGG pathway analysis. The cutoff of p value was defined as <0.05 for both GO and KEGG pathway analysis. Categories of gene ontology consisted of biological process (BP), cell component (CC) and molecular function (MF).

Investigating prognostic DEGs

Cox proportional hazards regression analysis of DEGs was carried out basing on data from TCGA through the online tool GEPIA2. Cutoff of adjusted p value was defined as <0.05 . For overall survival analysis, cohorts were grouped into high and low expressions of DEGs using the median expressions. Kaplan-Meier survival plots were drawn and Log-rank test were employed. Cutoff of p values was defined as <0.05 . For tumor stages analysis, cohorts were grouped by TNM stage and One way ANOVA was adopted. Cutoff of p value was defined as <0.05 .

Exploring interaction networks of DEGs

The corresponding proteins of DEGs were analyzed according to interaction frequency and interaction intensity through an online protein database String (string-db.org/). The minimum required interaction score was set to >0.04 and protein-protein interaction (PPI) networks were generated. PPI networks were visualized by Cytoscape (version 3.8.2). The expressions of corresponding proteins of DEGs in paraffin embedded samples were validated via The Human Protein Atlas (www.proteinatlas.org/).

Immune cell infiltration analysis

Tumor infiltrating lymphocytes (TILs) in pancreatic cancer were investigated using an online tool (cis.hku.hk/TISIDB/). The correlations between mRNA expressions of MARCO and abundance of TILs in pancreatic cancer were analyzed by Spearman correlation test. The cutoff of p value was defined as <0.01 .

Gene set enrichment analysis

The primary tumors of pancreatic cancer from TCGA were separated into group PCSK6_high and group PCSK6_low according to the median expression of PCSK6. Hallmark gene sets (including 50 gene sets) from Molecular Signatures Database (MSigDB v7.4 www.gsea-msigdb.org/gsea/msigdb) were used to performed Gene sets enrichment analysis (GSEA) between group PCSK6_high and group PCSK6_low. Normalized Enrichment Score (NES) was generated and normalized p value of gene set <0.05 was considered statistically significant.

Results

Microarray data information

181 data serials in total were collected from GEO, among which 8 data serials (Supplementary table 1) included samples of both primary tumor and adjacent normal tissue, and 2 data serials (GSE42952 and GSE71729) included samples of both hepatic metastasis and primary tumor (table 1).

Data serials GSE42952 and GSE71729 were selected for following analysis. GSE42952 including 10 primary tumor samples and 7 hepatic metastasis samples from surgical resections, was processed on array platform GPL570. GSE71729 including 145 primary tumor samples and 25 hepatic metastasis samples from surgical resections, was processed on array platform GPL20769.

DEGs in hepatic metastasis of pancreatic cancer

Data serials GSE42952 and GSE71729 were analyzed through GEO2R and volcano plots of DEGs in each data serial were showed (figure 1A and 1B). 1490 DEGs were identified between group of hepatic metastasis and group of primary tumor in GSE42952, including 588 up-regulated and 902 down-regulated DEGs. 1053 DEGs were identified between group of hepatic metastasis and group of primary tumor in GSE71729, including 445 up-regulated and 608 down-regulated DEGs. The overlapped H-DEGs were obtained, including 217 up-regulated H-DEGs and 257 down-regulated H-DEGs (figure 1C and 1D).

Verifications of DEGs in primary tumor and cell lines of pancreatic cancer

Data of TCGA and GTEx was used to generate a DEGs list between group of primary tumor and group of adjacent normal tissue, and it was designated as primary tumor related DEGs (P-DEGs). Through a comparison between H-DEGs and P-DEGs, 40 out of 217 up-regulated H-DEGs were also found up-regulated in primary tumor compared to adjacent normal tissue, meanwhile 11 out of 257 down-regulated H-DEGs were also found down-regulated in primary tumor compared to adjacent normal tissue (figure 2).

As mesenchymal components of the samples would confuse the results of gene expressions in tumor cells, a verification step in cell lines of pancreatic cancer was carried out. 27 out of 40 up-regulated H-DEGs and 2 out of 11 down-regulated H-DEGs in previous step were verified (figure 3A and 3B). The finally generated H-DEGs were presented by heat plot (figure 3C). The expressing profiles of all cell lines were available in Supplementary table 2.

GO and KEGG pathway enrichment of DEGs

For GO analysis (table 2), negative regulation of blood coagulation, negative regulation of hemostasis, alcohol metabolic process and so on were the enrichment results of BP (figure 4A). Collagen-containing extracellular matrix, endoplasmic reticulum lumen, chylomicron and so on were the enrichment results of CC (figure 4B). Carboxylic acid binding, sulfur compound binding, vitamin binding and so on were the enrichment results of MF (figure 4C).

Complement and coagulation cascades, Arginine and proline metabolism, Steroid biosynthesis, and alanine, aspartate and glutamate metabolism were the enrichment results of KEGG pathway (table 4). The corresponding p values and H-DEGs in each KEGG pathway were presented (figure 4D and 4E).

Prognostic DEGs

For cox proportional hazards regression analysis, genes with $HR > 1$ were considered as factors promoting tumor progression, while genes with $HR < 1$ were considered as factors preventing tumor progression. 18 out of 27 up-regulated H-DEGs were found $HR > 1$, while none of 2 down-regulated H-DEGs was found $HR < 1$. Over-expressions of MARCO and PCSK6 among the 18 H-DEGs ($HR > 1$) were both significantly associated with decreased overall survivals ($p = 0.046$ and $P = 0.013$). Further analysis showed that MARCO and PCSK6 were both significantly correlated with TNM stages (figure 5).

PPI networks and orthotopic expressions of candidate DEGs

MARCO and PCSK6 were chosen as candidate DEGs to generate PPI networks through String and visualized by cytoscape (figure 6A). The PPI network of MARCO consisted of 11 nodes and 38 edges and the PPI network of PCSK6 consisted of 11 nodes and 16 edges. Each node represented a protein that would interact with MARCO or PCSK6.

The corresponding protein of MARCO and PCSK6 were examined by immunohistochemistry (figure 6B). The representative stainings of PCSK6 in pancreatic cancer, normal pancreas tissue and normal liver tissue were showed, while the stainings of MARCO were negative in current samples of pancreatic cancer, normal pancreas tissue and normal liver tissue in database of The Human Protein Atlas.

Expression of MARCO and TILs in pancreatic cancer

As the expression of MARCO might be related to TILs, correlation between mRNA expression of MARCO and 8 types of TILs including Neutrophil, Macrophage, natural killer cell (NK), myeloid derived suppressor cell (MDSC), regulatory T cell (Treg), activated B cell (Act_B), activated CD4 T cell (Act_CD4) and activated CD8 T cell (Act_CD8) in pancreatic cancer were analyzed (figure 6C). 5 types of TILs including Macrophage, MDSC, NK, Treg and Act_CD4 were positively correlated to expression of MARCO (p value < 0.01 and $\rho > 0$). Treg, MDSC, Macrophage, NK and Act_CD4 were ranked in decreasing order of ρ coefficients.

Functional gene sets correlated to expression of PCSK6

Totally 172 samples of pancreatic adenocarcinoma from TCGA were separated into group PCSK6_high ($n = 86$) and group PCSK6_low ($n = 86$). The enrichment list of gene sets (top 20) was ranked by NES (table 3). There were 9 significant gene sets (normalized $P < 0.05$) included Notch signaling, Mitotic spindle, TGF beta signaling, Glycolysis, Estrogen response early, Peroxisome, Estrogen response late, Apoptosis and P53 pathway. The enrichment plots of significant gene sets were showed (figure 7A). Top 50 genes in each group were plotted by heatmap (figure 7B). The correlations between NES and p value of gene sets were visualized (figure 7C).

Discussion

Liver was one of the most common sites that pancreatic cancer metastasized to and around 40-50% of the first admitted patients were found with hepatic metastasis, whose prognosis were extremely poor [12, 13]. Besides, hepatic metastasis arose early and frequently in patients even if curative resections of tumors had been performed [14–16]. It indicated that hepatic metastasis initiated at very early stage and tumor cells had already settled down in liver before operations, while no sign of hepatic metastasis would be found by radiologists. Therefore, it was challenged to improve overall survivals of patients with pancreatic cancer.

In this study we established a comparison between hepatic metastasis and primary tumor to explore DEGs, focusing on the genes associated with hepatic metastasis. We found 588 and 445 up-regulated genes in two data serials respectively, meanwhile 902 and 608 down-regulated genes were found respectively. Overlapped DEGs including 217 up-regulated H-DEGs and 257 down-regulated H-DEGs showed consistent differential expressions across two data serials.

Due to requirements for adaptations to different microenvironments, the transcriptional profiles within primary tumor might change within metastatic lesions of distant organs [17, 18]. If the H-DEGs showed differential expressions only in hepatic metastasis (compared to primary tumor), these H-DEGs known as passenger genes might accommodate the colonized tumor cells to a new microenvironment. Instead, if the H-DEGs showed differential expressions in both hepatic metastasis (compared to primary tumor) and primary tumor (compared to adjacent normal tissue), these H-DEGs known as driver genes might initiate metastasis, promote metastasis and establish tumor colonies in liver. In the latter condition, the colonized tumor cells in liver would show an enrichment of subclones from the primary tumor with driver H-DEGs.

The driver H-DEGs functioning in both primary tumor and hepatic metastatic lesion, would be promising therapeutic targets and diagnostic markers in pre-metastasis or post-metastasis timescale. Therefore, a further comparison between H-DEGs and P-DEGs was undertaken to explore the driver H-DEGs. Subsequently a verification in CCLE database was adopted to minimize the influence of mesenchymal components in the tissue samples. Totally, 27 up-regulated H-DEGs and 2 down-regulated H-DEGs were obtained.

It revealed that the H-DEGs participated in serials of biological regulations including regulation of coagulation, lipid metabolism, secretion of particles and amino acid metabolism through GO and KEGG pathway analysis, instead of classical processes such as cell proliferation, apoptosis, cell migration, EMT and so on in previous studies [19, 20]. Reprogramming of tumor metabolism played a significant role in tumor metastasis [21, 22]. Plenty of tumor metabolism related genes had been discovered [23–26]. Among the H-DEGs, iron metabolism related genes including GOT1 and CP [27, 28], glutamine metabolism related gene GOT1 [29], pyruvate metabolism related gene PC [30], proline metabolism related gene ALDH4A1 [31], and so on were found in this study. Alterations of tumor metabolism including shift of energy source, glucose metabolism through pentose phosphate pathway, lipid synthesis, increase of glutamine consumption and regulations of redox, were compatible with variations

of tumor microenvironment, to meet the demands for metastasis. Tumor metabolism related H-DEGs in this study might be a novel sight in hepatic metastasis of pancreatic cancer.

In current study MARCO and PCSK6 were found to be prognostic genes. MARCO was a receptor with collagenous structure, related to removal of pathogens and tumor progression, however it was mainly expressing on macrophage subset [32]. It was unclear whether MARCO functioned in mesenchymal cells, tumor cells, or both during the process of hepatic metastasis in pancreatic cancer. No obvious staining of MARCO protein was found in pancreatic cancer and it was consistent to the result that most of the cell lines of pancreatic cancer didn't express MARCO except BxPC-3 in this study. It indicated that up-regulation of MARCO in pancreatic cancer might attribute to mesenchymal components. Tumor infiltrating lymphocytes in tumor microenvironment were analyzed in this study. Treg, MDSC and Macrophage were the top three TILs correlated to up-regulation of MARCO in pancreatic cancer. We subsequently established a PPI interaction network including MARCO and 10 predicted proteins. VSIG4 was a B7 family-related macrophage protein and promoted tumor progression by inhibiting T cell activation [33]. C1QA, C1QB and C1QC were correlated to immune activity of tumor microenvironment and influenced patient's survivals [34, 35]. These evidences suggested MARCO might play a role in regulating tumor immune microenvironment and more investigations would be needed.

PCSK6 was one member of the novel family of proprotein convertases, Ca^{2+} dependent serine proteases, which were capable of processing various protein precursors into their active products, including hormones, tyrosine phosphatases, growth factors, metalloproteinases and adhesion molecules [36]. PCSK6 had been found involving in migration of smooth muscle cells and multiple biological behaviors of tumor cells [37–39], but the role of PCSK6 in tumor metastasis especially hepatic metastasis remained elusive. In this study PCSK6 was found up-regulated in hepatic metastasis of pancreatic cancer and over-expression of PCSK6 was correlated to decreased overall survivals. Significant staining of PCSK6 was verified in pancreatic cancer and it was mainly expressing in cytoplasm of tumor cells, in accordance with that PCSK6 was expressing in 10 out of 13 cell lines of pancreatic cancer. Among the PPI interaction network of PCSK6, NGF a nerve growth factor secreted from pancreatic cancer cells and stellate cells was identified as a promising therapeutic target in pancreatic cancer [40, 41]. Inhibiting PCSK9 increased the expression of MHC I on tumor cell surface and promoted intra-tumor infiltration of cytotoxic T cells, potentially enhancing immune checkpoint therapy [42]. Proprotein convertases participated in the process of lipid metabolism and regulated clearance of plasma low density lipoprotein [43]. Notch signaling, Mitotic spindle, TGF beta signaling, Glycolysis and Estrogen response early were the top 5 gene sets generated by the GSEA analysis in this study, indicating that over-expression of PCSK6 was correlated to activations of these biological process in pancreatic cancer. Therefore, up-regulation of PCSK6 might activate various enzymes, substrates, receptors, chemokines and transcription factors contributing to regulation of critical signaling pathway and reprogramming of tumor metabolism, leading to hepatic metastasis, but elucidations of detailed mechanisms would be needed in the future.

Conclusions

In this study two data serials with samples of hepatic metastasis and primary tumor in pancreatic cancer were chosen to generate a cluster of hepatic metastasis related DEGs. These H-DEGs were further verified using samples of tumor tissue and cell lines of pancreatic cancer in public database. Totally 27 up-regulated and 2 down-regulated H-DEGs were obtained. The enrichment results of GO and KEGG pathway analysis showed reprogramming of tumor metabolism might play a role in hepatic metastasis of pancreatic cancer. Among the H-DEGs, MARCO and PCSK6 were prognostic genes and correlated to tumor immune microenvironment and reprogramming of tumor metabolism. The H-DEGs without significant prognostic indications obtained in this study were also deserved to further explorations. However, there were limitations in this study and further investigations might be performed to find out the detailed mechanism how these H-DEGs regulated hepatic metastasis of pancreatic cancer.

Declarations

Funding

This study was supported by Chinesisch-Deutsche Kooperationsgruppe: Precision Medicine in Pancreatic Cancer (Grant No. GZ 1456)

Author Contributions

Hang He designed the study and drafted the manuscript. Minrui Liang analyzed the results and revised the manuscript.

Competing interests

The authors declared that they had no relevant financial or non-financial interests.

Data availability

The original findings of current study were presented in the article and further inquiries will be available from the corresponding author.

Ethics approval

Ethical review and approval were not required in this study.

References

1. Sung H et al (2021) Global Cancer Statistics 2020: GLOBOCAN Estimates of Incidence and Mortality Worldwide for 36 Cancers in 185 Countries. *CA Cancer J Clin* 71(3):209–249
2. Siegel RL et al (2021) *Cancer Statistics*, *CA Cancer J Clin*, 2021. 71(1): p. 7-33
3. Kneuert PJ et al (2011) Palliative surgical management of patients with unresectable pancreatic adenocarcinoma: trends and lessons learned from a large, single institution experience. *J*

Gastrointest Surg 15(11):1917–1927

4. Giovannetti E et al (2017) Never let it go: Stopping key mechanisms underlying metastasis to fight pancreatic cancer. *Semin Cancer Biol* 44:43–59
5. Pavlidis ET, Pavlidis TE (2018) Current Molecular and Genetic Aspects of Pancreatic Cancer, the Role of Metastasis Associated Proteins (MTA): A Review. *J Invest Surg* 31(1):54–66
6. Shi H, Li J, Fu D (2016) Process of hepatic metastasis from pancreatic cancer: biology with clinical significance. *J Cancer Res Clin Oncol* 142(6):1137–1161
7. Nakamura T, Fidler IJ, Coombes KR (2007) Gene expression profile of metastatic human pancreatic cancer cells depends on the organ microenvironment. *Cancer Res* 67(1):139–148
8. Moffitt RA et al (2015) Virtual microdissection identifies distinct tumor- and stroma-specific subtypes of pancreatic ductal adenocarcinoma. *Nat Genet* 47(10):1168–1178
9. Yu S et al (2020) Plasma extracellular vesicle long RNA profiling identifies a diagnostic signature for the detection of pancreatic ductal adenocarcinoma. *Gut* 69(3):540–550
10. McDonald OG et al (2017) Epigenomic reprogramming during pancreatic cancer progression links anabolic glucose metabolism to distant metastasis. *Nat Genet* 49(3):367–376
11. Ren B et al (2018) Tumor microenvironment participates in metastasis of pancreatic cancer. *Mol Cancer* 17(1):108
12. Maire F et al (2017) Epidemiology of pancreatic cancer in France: descriptive study from the French national hospital database. *Eur J Gastroenterol Hepatol* 29(8):904–908
13. van der Geest LGM et al (2017) Nationwide outcomes in patients undergoing surgical exploration without resection for pancreatic cancer. *Br J Surg* 104(11):1568–1577
14. Tanaka M et al (2019) Meta-analysis of recurrence pattern after resection for pancreatic cancer. *Br J Surg* 106(12):1590–1601
15. Dreyer SB et al (2021) Genomic and molecular analyses identify molecular subtypes of pancreatic cancer recurrence. *Gastroenterology*,
16. Imamura M et al (2021) *Perioperative Predictors of Early Recurrence for Resectable and Borderline-Resectable Pancreatic Cancer*. *Cancers (Basel)*, **13**(10)
17. Herting CJ, Karpovsky I, Lesinski GB (2021) The tumor microenvironment in pancreatic ductal adenocarcinoma: current perspectives and future directions. *Cancer Metastasis Rev* 40(3):675–689
18. Truong LH, Pauklin S (2021) *Pancreatic Cancer Microenvironment and Cellular Composition: Current Understandings and Therapeutic Approaches*. *Cancers (Basel)*, **13**(19)
19. Crawford HC, Pasca di M, Magliano, Banerjee S (2019) Signaling Networks That Control Cellular Plasticity in Pancreatic Tumorigenesis, Progression, and Metastasis. *Gastroenterology* 156(7):2073–2084
20. Javadrashid D et al (2021) *Pancreatic Cancer Signaling Pathways, Genetic Alterations, and Tumor Microenvironment: The Barriers Affecting the Method of Treatment*. *Biomedicines*, **9**(4)

21. Brown RAM et al (2020) Altered Iron Metabolism and Impact in Cancer Biology, Metastasis, and Immunology. *Front Oncol* 10:476
22. Bergers G, Fendt SM (2021) The metabolism of cancer cells during metastasis. *Nat Rev Cancer* 21(3):162–180
23. Liu RZ, Godbout R (2020) *An Amplified Fatty Acid-Binding Protein Gene Cluster in Prostate Cancer: Emerging Roles in Lipid Metabolism and Metastasis*. *Cancers (Basel)*, 12(12)
24. Nie S et al (2020) ALDH1A3 Accelerates Pancreatic Cancer Metastasis by Promoting Glucose Metabolism. *Front Oncol* 10:915
25. Nacke M et al (2021) An ARF GTPase module promoting invasion and metastasis through regulating phosphoinositide metabolism. *Nat Commun* 12(1):1623
26. Sandoval-Acuna C et al (2021) Targeting Mitochondrial Iron Metabolism Suppresses Tumor Growth and Metastasis by Inducing Mitochondrial Dysfunction and Mitophagy. *Cancer Res* 81(9):2289–2303
27. Shang Y et al (2020) Ceruloplasmin suppresses ferroptosis by regulating iron homeostasis in hepatocellular carcinoma cells. *Cell Signal* 72:109633
28. Kremer DM et al (2021) GOT1 inhibition promotes pancreatic cancer cell death by ferroptosis. *Nat Commun* 12(1):4860
29. Abrego J et al (2017) GOT1-mediated anaplerotic glutamine metabolism regulates chronic acidosis stress in pancreatic cancer cells. *Cancer Lett* 400:37–46
30. Cheng T et al (2011) Pyruvate carboxylase is required for glutamine-independent growth of tumor cells. *Proc Natl Acad Sci U S A* 108(21):8674–8679
31. Lorenzo C et al (2021) ALDH4A1 is an atherosclerosis auto-antigen targeted by protective antibodies. *Nature* 589(7841):287–292
32. Kraal G et al (2000) The macrophage receptor MARCO. *Microbes Infect* 2(3):313–316
33. Liao Y et al (2014) VSIG4 expression on macrophages facilitates lung cancer development. *Lab Invest* 94(7):706–715
34. Azzato EM et al (2010) Common germ-line polymorphism of C1QA and breast cancer survival. *Br J Cancer* 102(8):1294–1299
35. Chen LH et al (2021) Complement C1q (C1qA, C1qB, and C1qC) May Be a Potential Prognostic Factor and an Index of Tumor Microenvironment Remodeling in Osteosarcoma. *Front Oncol* 11:642144
36. Bassi DE, Mahloogi H, Klein-Szanto AJ (2000) The proprotein convertases furin and PACE4 play a significant role in tumor progression. *Mol Carcinog* 28(2):63–69
37. Bassi DE et al (2015) Enhanced aggressiveness of benzopyrene-induced squamous carcinomas in transgenic mice overexpressing the proprotein convertase PACE4 (PCSK6). *Mol Carcinog* 54(10):1122–1131

38. Rykaczewska U et al (2020) PCSK6 Is a Key Protease in the Control of Smooth Muscle Cell Function in Vascular Remodeling. *Circ Res* 126(5):571–585
39. Weishaupt C et al (2020) Paired Basic Amino Acid-cleaving Enzyme 4 (PCSK6): An Emerging New Target Molecule in Human Melanoma. *Acta Derm Venereol* 100(10):adv00157
40. Lei Y et al (2017) Gold nanoclusters-assisted delivery of NGF siRNA for effective treatment of pancreatic cancer. *Nat Commun* 8:15130
41. Jiang J et al (2020) NGF from pancreatic stellate cells induces pancreatic cancer proliferation and invasion by PI3K/AKT/GSK signal pathway. *J Cell Mol Med* 24(10):5901–5910
42. Liu X et al (2020) Inhibition of PCSK9 potentiates immune checkpoint therapy for cancer. *Nature* 588(7839):693–698
43. Guo S et al (2020) Proprotein Convertase Subtilisin/Kexin-Type 9 and Lipid Metabolism. *Adv Exp Med Biol* 1276:137–156

Tables

Table 1 Characteristics of data serials

GSE accession	Platform	Primary tumor sample	Hepatic metastasis sample	Total sample count	Author and year	Region
GSE42952	GPL570	12	7	19	Van et al. 2013	Belgium
GSE71729	GPL20769	145	25	170	Moffitt et al. 2015	USA

Table 2 Enrichment results of Gene ontology and KEGG pathway analysis

Gene ontology				
ID	Term	Counts	p value	p.adjust
BP GO:0030195	negative regulation of blood coagulation	4	7.225277e-07	2.5310485637854336E-7
BP GO:1900047	negative regulation of hemostasis	4	7.859513e-07	3.072740394980281E-5
BP GO:0006066	alcohol metabolic process	7	9.251975e-07	6.220193186222314E-5
BP GO:0050819	negative regulation of coagulation	4	1.001186e-06	0.008757875763815318
BP GO:0030193	regulation of blood coagulation	4	2.627600e-06	0.028841147257816065
CC GO:0062023	collagen-containing extracellular matrix	7	2.206726e-06	0.0001699179
CC GO:0005788	endoplasmic reticulum lumen	5	7.989218e-05	0.0030758488
CC GO:0042627	chylomicron	2	1.645535e-04	0.0042235409
CC GO:0034361	very-low-density lipoprotein particle	2	3.982579e-04	0.0061331709
CC GO:0034385	triglyceride-rich plasma lipoprotein particle	2	3.982579e-04	0.0061331709
MF GO:0031406	carboxylic acid binding	5	9.409521e-06	0.001270285
MF GO:1901681	sulfur compound binding	5	4.956788e-05	0.003345832
MF GO:0019842	vitamin binding	4	7.638880e-05	0.003437496
MF GO:0008201	heparin binding	4	1.230388e-04	0.003645488
MF GO:0004252	serine-type endopeptidase activity	4	1.350181e-04	0.003645488
KEGG pathway				
ID	Term	Counts	p value	p.adjust
hsa04610	Complement and coagulation cascades	5	2.014017e-06	8.861673e-05

hsa00330	Arginine and proline metabolism	3	2.886443e-04	6.350174e-03
hsa00100	Steroid biosynthesis	2	1.182373e-03	1.734147e-02
hsa00250	Alanine, aspartate and glutamate metabolism	2	4.035996e-03	4.439595e-02

Table 3 Ranked list of gene sets (top 20)

NAME	SIZE	ES	NES	NOM p-val	FDR q-val
NOTCH_SIGNALING	32	0.655	1.947	0.000	0.020
MITOTIC_SPINDLE	199	0.613	1.897	0.004	0.023
TGF_BETA_SIGNALING	54	0.655	1.883	0.004	0.020
GLYCOLYSIS	200	0.508	1.703	0.012	0.109
ESTROGEN_RESPONSE_EARLY	200	0.437	1.685	0.000	0.105
PEROXISOME	104	0.478	1.673	0.006	0.097
PROTEIN_SECRETION	96	0.555	1.610	0.064	0.137
INTERFERON_ALPHA_RESPONSE	97	0.652	1.574	0.057	0.154
ESTROGEN_RESPONSE_LATE	200	0.399	1.552	0.013	0.156
G2M_CHECKPOINT	200	0.572	1.546	0.090	0.148
APOPTOSIS	161	0.436	1.531	0.040	0.149
ANDROGEN_RESPONSE	100	0.460	1.524	0.076	0.140
P53_PATHWAY	200	0.393	1.490	0.022	0.161
MTORC1_SIGNALING	200	0.471	1.439	0.110	0.200
APICAL_JUNCTION	199	0.388	1.423	0.083	0.206
E2F_TARGETS	200	0.527	1.376	0.189	0.251
XENOBIOTIC_METABOLISM	199	0.351	1.376	0.060	0.237
APICAL_SURFACE	44	0.407	1.357	0.091	0.244
FATTY_ACID_METABOLISM	157	0.385	1.356	0.130	0.233
INTERFERON_GAMMA_RESPONSE	200	0.479	1.313	0.220	0.267

Figures

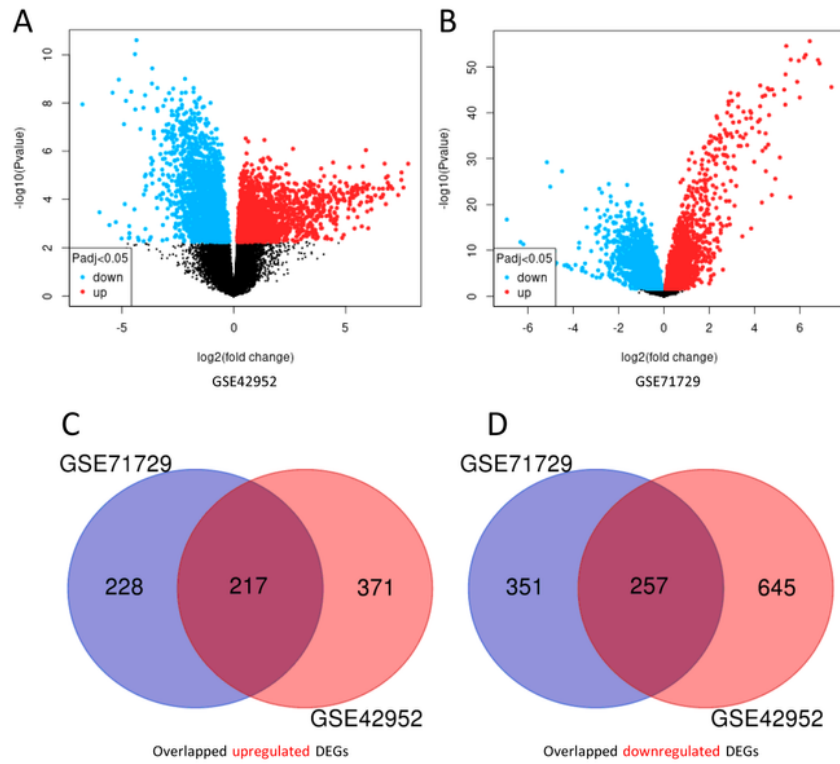


Figure 1

DEGs in data serials

Red points represented up-regulated DEGs. Blue points represented down-regulated DEGs. Black points represented genes with adjusted p value >0.05 A: Volcano plot of DEGs in GSE42952 B: Volcano plot of DEGs in GSE71729 C: Overlapped up-regulated DEGs across data serials D Overlapped down-regulated DEGs across data serials

Figure 2

mRNA expressions of DEGs in pancreatic cancer

DEGs were verified using TCGA and GTEx data including 179 primary tumor samples and 171 adjacent normal tissue samples. Totally 40 up-regulated DEGs and 11 down-regulated DEGs were showed in this plot with adjusted p value <0.01 and $\text{Log}_2 \text{FC} \geq 1$ or ≤ -1 . Red box represented the mRNA expressions in primary tumor. Gray box represented the mRNA expressions in adjacent normal tissues. PAAD represented pancreatic adenocarcinoma.

Figure 3

mRNA expressions of DEGs in cell lines of pancreatic cancer

A: Counts of cell lines with expressions of DEGs over cutoff value ($\text{Log}_2(\text{TPM}+1) > 2$). The x-axis indicated the counts of cell lines. The y-axis indicated each of DEGs. B: Average expressions of DEGs in corresponding cell lines. The x-axis indicated the average expressing values $\text{Log}_2(\text{TPM}+1)$. The y-axis indicated each of DEGs. C: Heat plot of verified H-DEGs. Met.A and Pri.A represented group of hepatic metastasis and group of primary tumor respectively in GSE71729. Met.B and Pri.B represented group of hepatic metastasis and group of primary tumor respectively in GSE42952.

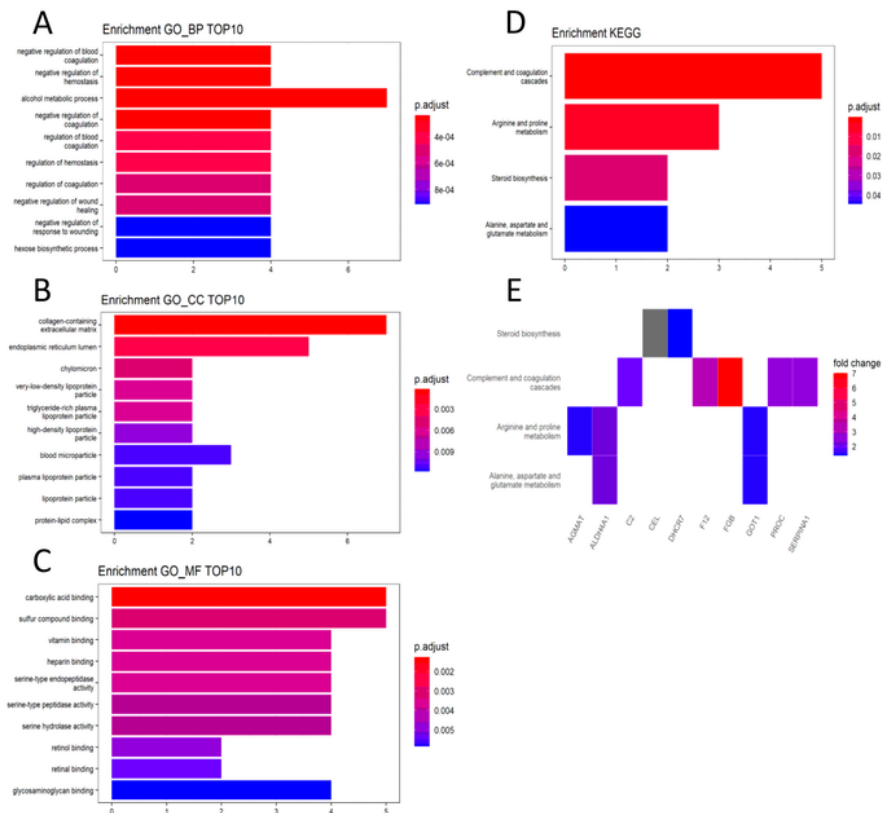


Figure 4

GO and KEGG pathway analysis

A: Top 10 enrichment results of biological process (BP) B: Top 10 enrichment results of cell component (CC) C: Top 10 enrichment results of molecular function (MF) D: Enrichment results of KEGG pathway E: Fold change of DEGs in each KEGG pathway. The x-axis indicated counts of DEGs in A, B, C and D.

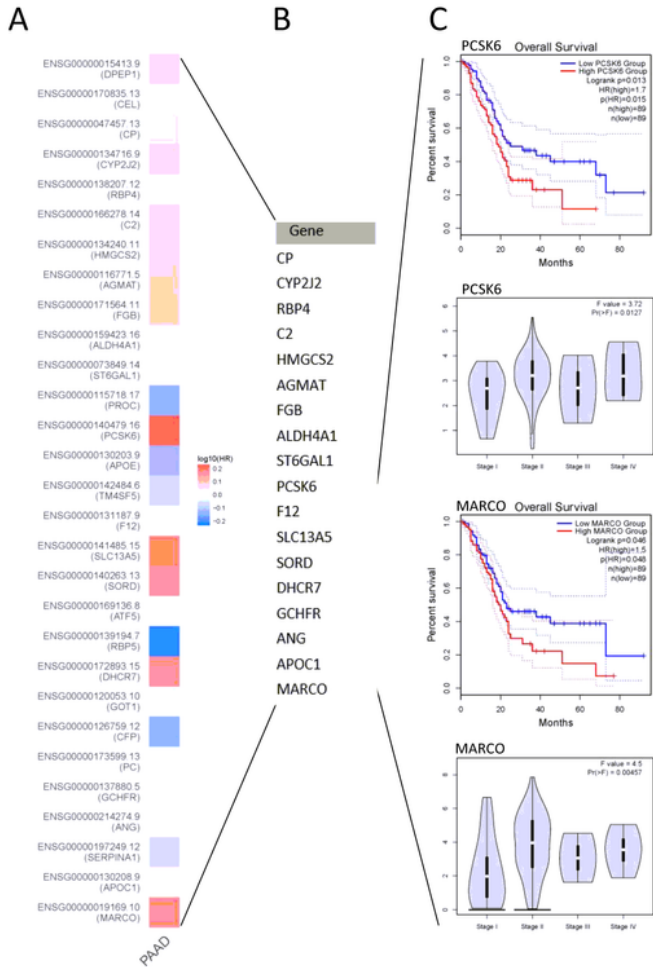


Figure 5

Prognostic DEGs

A: Cox proportional hazards regression analysis. $\log_{10}(\text{HR}) > 0$ indicated the genes promoting tumor progression and $\log_{10}(\text{HR}) < 0$ indicated the genes preventing tumor progression. B: 18 up-regulated H-DEGs were found $\text{HR} > 1$ or $\log_{10}(\text{HR}) > 0$. C: Kaplan-Meier survival plots and Log-rank test of MARCO

($p=0.046$) and PCSK6 ($P=0.013$). Correlations between mRNA expressions of MARCO ($p=0.00457$) or PCSK6 ($p=0.0127$) and TNM stage.

Figure 6

Functions and expressions of MARCO and PCSK6

A: PPI networks of MARCO and PCSK6. The red node represented MARCO protein or PCSK6 protein. The yellow nodes represented the target proteins interacting with MARCO or PCSK6. The lines represent interactions between proteins. B: Immunohistochemistry stainings of MARCO and PCSK6 proteins in pancreatic cancer, normal pancreas tissue and normal liver tissue. C: Correlations between expression of MARCO and TILs in pancreatic cancer. P value <0.01 indicated significant correlation. The x-axis indicated mRNA expression of MARCO. The y-axis indicated the abundance of TILs.

Figure 7

Gene set enrichment analysis of PCSK6

A: Enrichment plots of significant gene sets. Group setting was defined as PCSK6_high versus PCSK6_low. Each plot represented a single gene set with p value <0.05 . B: Heatmap of top 50 genes in all gene sets between group PCSK6_high and group PCSK6_low. C: correlations between normalized enrichment score (NES) and p value of gene sets. X axis represented NES. Left Y axis represented q value. Right Y axis represented nominal p value.

Supplementary Files

This is a list of supplementary files associated with this preprint. Click to download.

- [supplementarytable1.docx](#)
- [supplementarytable2.docx](#)